Phase Relations, Crystal Structure, and Electron Transport Properties of Phosphate Tungsten Bronzes $(K_xNa_y)(PO_2)_4(WO_3)_{2m}$ ($m = 4, 6$)

Pascal Roussel,* Daniel Groult, Antoine Maignan, and Philippe Labbé

Laboratoire CRISMAT, UMR 6508 associée au CNRS, ISMRA et Université de Caen 6, Boulevard Maréchal Juin, 14050 CAEN Cedex—France

Received December 10, 1998. Revised Manuscript Received April 6, 1999

Phase relations in the system Na−K−P−W−O have been studied for two values $m = 4$ and $m = 6$ of the relevant parameter m which characterizes the thickness of the perovskite WO_3-type slabs within the series of the low dimensional tungsten phosphate bronzes $(K_xNa_y)(PO_2)_4(WO_3)_{2m}$. New $Na_yP_4W_{12}O_{44}$ bronzes ($0 \leq y \leq 1$) belonging to the monophosphate tungsten bronzes with pentagonal tunnels family have been isolated and studied by single-crystal X-ray diffraction and resistivity measurements. The crystal structure of $Na_{0.96}P_4W_{12}O_{44}$ has been solved and refined to conventional $R = 0.0289$ (w$R = 0.0414$) with 2924 reflections with $I \geq 3\sigma(I)$. Like that of $P_4W_{12}O_{44}$, the unit cell is orthorhombic (space group $P2_12_12_1$) with $a = 5.3083(3)$ Å, $b = 6.5790(7)$ Å, and $c = 23.6360(10)$ Å. The location of Na^+ cations in the O_{18} cages with pentagonal windows is compared to that of Na^+ cations in the O_{18} cages with hexagonal windows of the monophosphate tungsten bronzes with hexagonal tunnels $Na_{1.7}P_4W_{12}O_{44}$. Electron transport properties of single crystals of both monophosphate tungsten bronzes with pentagonal and hexagonal tunnels are described and discussed in terms of possible charge density wave (CDW) instabilities.

Introduction

In recent years several studies have been focused on the chemical aspects and the physical properties of families of transition metal oxides, chalcogenides, and bronzes showing quasi-one (1D) or -two-dimensional (2D) electronic properties.[1−3] In this context the **p**hosphate **t**ungsten **b**ronzes (PTB) $A_x(PO_2)_4(WO_3)_{2m}$ have been shown to form a huge family of low dimensional metallic materials with electronic instabilities of charge density wave (CDW) type.[4−9] In fact, four series of compounds must be distinguished even if the structures obey a similar elementary building principle which involves WO_3 octahedral slabs of perovskite ReO_3-type linked together through tetrahedral slices of PO_4 or P_2O_7 groups.[10,11] The first type corresponds to the so-called **di**phosphate **t**ungsten **b**ronzes with **h**exagonal tunnels (DPTBh) which are formed when the size of the guest cation, A, is larger or equal to that of K^+ ($A = K^+$, Rb^+, Tl^+, Ba^{2+}).[12,13] If the cation is Cs^+, a second type of structure is obtained which differs from the former by the existence of wide tunnels of octagonal form inside which Cs^+ cations are located.[14] In contrast, when the size of the A cation is smaller or equal to that of K^+ ($A = K^+$, Na^+, Pb^{2+}), a third series of compounds is isolated and called **m**ono**p**hosphate **t**ungsten **b**ronzes with **h**exagonal tunnels (MPTBh) which have the same formula as DPTBh's $A_x(PO_2)_4(WO_3)_{2m}$ but present a change in the orientation of the WO_3 octahedral slabs which are now connected by means of PO_4 tetrahedra instead of diphosphate P_2O_7 groups.[15−17] The fourth series of PTB is represented by the so-called **m**ono**p**hosphate **t**ungsten **b**ronzes with **p**entagonal tunnels (MPTBp) whose formula $(PO_2)_4(WO_3)_{2m}$ suggests that they are undoped compounds, i.e., without A cations in the tunnels. Like that of MPTBh's, the structure can be described as built

* Corresponding author e-mail address: p.roussel@crismat.ismra.fr.

(1) Rouxel, J., Ed. *Crystal chemistry and properties of materials with quasi one-dimensional structures*; Kluwer Academic Publisher: Dordrecht, 1986.
(2) Schlenker, C., Ed. *Low dimensional electronic properties of molybdenum bronzes and oxides*; Kluwer Academic Publisher: Dordrecht, 1989.
(3) Schlenker, C., Dumas, J., Greenblatt, M., van Smaalen, S., Ed.; *Physics and chemistry of low dimensional inorganic conductors*; NATO ASI Series B354; Plenum Press Publisher: New York, 1996.
(4) Wang E.; Greenblatt M.; Rachidi, I. E.; Canadell, E.; Whangbo, M. H.; Vadlamannati, S. *Phys. Rev.* **1989**, *B 39*, 12969.
(5) Teweldemedhin, Z. S.; Ramanujachary, K. V.; Greenblatt, M. *Phys. Rev.* **1992**, *B46*, 7897.
(6) Wang E.; Greenblatt M.; Rachidi, I. E.; Canadell, E.; Whangbo, M. H. *Inorg. Chem*. **1989**, *28*, 2451.
(7) Canadell, E.; Whangbo, M. H. *Phys. Rev*. **1991**, *B43*, 1894.
(8) Hess, C.; Schlenker, C.; Dumas, J.; Greenblatt, M.; Teweldemedhin, Z. S. *Phys. Rev.* **1996**, *B54*, 4581.
(9) Schlenker, C.; Hess, C.; Letouze, C.; Dumas, J. *J. Phys. I (Schegolev Memorial Volume)* **1996**, *6*, 2061.
(10) Raveau B. *Proc. Indian Natl. Sci. Acad*. **1986**, *52A*, 67.
(11) Labbé, Ph. In *Diffusionless phase transitions and related structures in oxides*; Boulesteix, C., Ed. Trans. Tech. Publications: Switzerland, 1992.
(12) Giroult, J. P.; Goreaud, M.; Labbé, Ph.; Raveau, B. *Acta Crystallogr.* **1982**, *B38*, 2342.
(13) Lamire, M.; Labbé, Ph.; Goreaud, M.; Raveau, B. *J. Solid State Chem*. **1987**, *71*, 342.
(14) Goreaud, M.; Labbé, Ph.; Raveau, B. *J. Solid State Chem*. **1985**, *56*, 41.
(15) Giroult, J. P.; Goreaud, M.; Labbé, Ph.; Raveau, B. *J. Solid State Chem*. **1982**, *44*, 407.
(16) Benmoussa, A.; Groult, D.; Labbé, Ph.; Raveau, B. *Acta Crystallogr.* **1984**, *C40*, 573.
(17) Roussel P.; Masset, A. C.; Domengès, B.; Maignan, A.; Groult, D.; Labbé, Ph. *J. Solid State Chem*. **1998**, *139*, 362.

10.1021/cm9807790 CCC: $18.00
Published on Web 07/10/1999

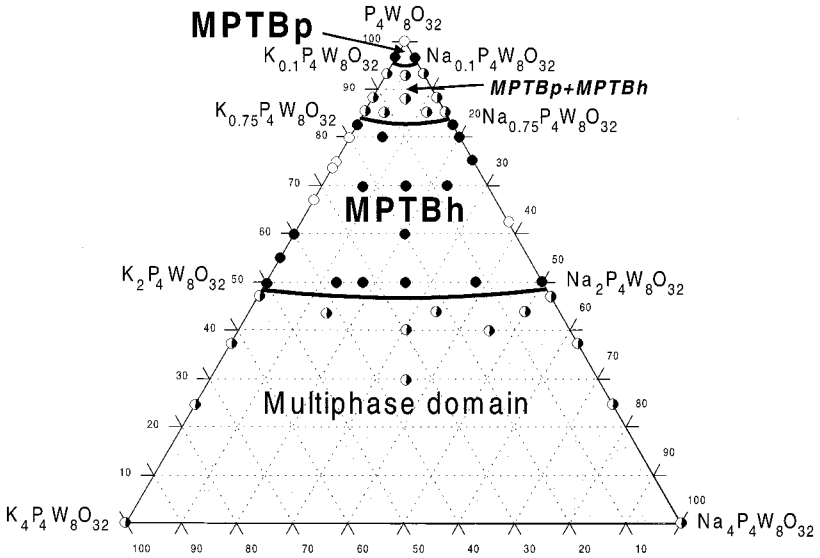

Figure 1. Stability phase domains of phosphate tungsten bronzes $(K_xNa_y)P_4W_8O_{32}$. The filled circles correspond to pure phases and half filled circles to multiphased samples involving mixtures of MPTBh's with MPTBp's or other members of the series and tungsten bronzes A_xWO_3 (A = K, Na). The thick lines are guides for the eyes. Note that empty circles correspond to previous phase compositions of single crystals used for X-ray structure determinations (refs 15, 16, and 18) or resistivity measurements (refs 5, 23, and 30).

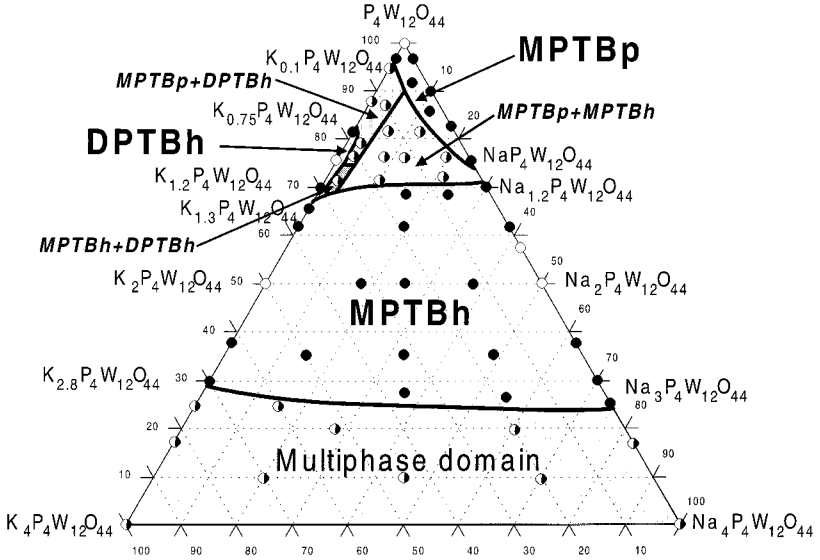

Figure 2. Stability phase domains of phosphate tungsten bronzes $(K_xNa_y)P_4W_{12}O_{44}$. The filled circles correspond to pure phases and half filled circles to multiphased samples. Note that empty circles correspond to previous phase compositions of single crystals used for X-ray structure determinations (refs 16, 19, and 26) or resistivity measurements (refs 4, 6, 26, and 30). The thick lines are guides for the eyes.

from parallel ReO_3-type layers of corner-sharing WO_6 octahedra linked through PO_4 tetrahedra.[18−20]

From a physical point of view this last series of compounds has been more extensively studied than the others and demonstrated to exhibit quasi-two-dimensional (2D) metallic properties with a Peierls transition toward a CDW state.[3−5,8,9] Moreover, because it offers the possibility to change the thickness of the conducting layers by changing the m value ($4 \leq m \leq 14$), the series has been considered by physicists as a model system to investigate how the CDW instability evolves when the number of conduction electrons per W atom $2/m$ is changed. It has thus been shown that for low m values ($m = 4$, 6) the critical CDW wave vector can be understood in the framework of a new Fermi surface nesting mechanism[21] while for large m values ($m \geq 8$) the CDW instability appears to compete with the antiferroelectric instability of pure WO_3 for which the thickness parameter becomes $m = \infty$.[22] More recently similar electron instabilities have been observed for the MPTBh member $K_xP_4W_8O_{32}$ ($m = 4$) with a critical temperature showing a maximum value $T_c \approx 170$ K for $x \approx 4/3$.[23,24] According to band structure calculations

(18) Giroult, J. P.; Goreaud, M.; Labbé, Ph.; Raveau, B. *Acta Crystallogr.* **1981**, *B37*, 2139.
(19) Labbé, Ph.; Goreaud, M.; Raveau, B. *J. Solid State Chem.* **1986**, *61*, 324.
(20) Roussel, P.; Labbé, Ph.; Groult, D.; Domengès, B.; Leligny, A.; Grebille, D. *J. Solid State Chem.* **1996**, *122*, 281.
(21) Whangbo, M. H.; Canadell, E.; Foury, P.; Pouget, J. P. *Science* **1991**, *252*, 96.
(22) Ottolenghi, A.; Pouget, J. P. *J. Phys. I Fr.* **1996**, *6*, 1059.
(23) Roussel, P.; Groult, D.; Hess, C.; Labbé, Ph.; Schlenker, C. *J. Phys. Condens. Matter.* **1997**, *9*, 7081.

Table 1. Crystallographic Data Concerning $Na_{0.96}P_4W_{12}O_{44}$[a]

chemical formula	$Na_{0.96}P_4W_{12}O_{44}$
chemical formula weight	3056.02
space group	$P2_12_12_1$ (no. 19)
a (Å)	5.3083(3)
b (Å)	6.5790(7)
c (Å)	23.636(1)
V (Å^3) ($Z = 1$)	825.4 (1)
density (g cm^{-3})	6.148
crystal size (mm^3)	0.26 × 0.19 × 0.06
F(000)	1311
diffractometer	Enraf Nonius CAD4
radiation	Kα Mo ($\lambda = 0.71073$ Å)
monochromator	oriented graphite (002)
scan mode	$\omega - \theta/2$
scan (deg)	$1 + 0.35 \tan\theta$
recording range θ (deg)	$2 \le \theta \le 45$
range of h, k, l	$-10 \le h \le 10$; $0 \le k \le 13$; $0 \le l \le 46$
no. of recorded reflections	7292
no. of independent reflections	3901
R_{int}	0.028
absorption correction	Gaussian method
linear absorption coefficient (cm^{-1})	419.6
T_{min}	0.012
T_{max}	0.138
no. of independent reflections with $I > 3.0\sigma(I)$ (N)	2924
weighting scheme	unit
R (%)	0.0289
wR (%)	0.0414
S	1.56
no. of refined parameters (M)	147
$(\Delta/\sigma)_{max}$	0.0007
extinction coefficient	1.69(3)

[a] $R = \sum||Fo| - |Fc||/\sum|Fo|$. w$R = [\sum w(|Fo| - |Fc|)^2/\sum w|Fc|^2]^{1/2}$. $S = [\sum w(|Fo| - |Fc|)^2/(N - M)]^{1/2}$. Isotropic secondary extinction (Type II) Gaussian distribution (ref 31).

(performed for $x = 0.8$[7]) the T_c dependence with x suggests that the relative filling of the three bands crossing the Fermi level varies with x but is associated with strong electron−lattice couplings inducing a lock-in-type transition. However, in the present state of the physical data, it is not possible to clearly explain the origin of this coupled electronic and structural transition. Further work is thus needed, and more particularly, phase relations in the involved K−Na−P−W−O systems have to be well understood.

In this paper we report on the chemical and X-ray diffraction analysis of the K−Na−P−W−O diagrams for two relevant values $m = 4$ and $m = 6$ of the thickness parameter. The structure of new Na-doped MPTBp $Na_yP_4W_{12}O_{44}$ ($y \le 1$) is discussed, and the electron transport properties are compared with those of the undoped compound $P_4W_{12}O_{44}$ ($y = 0$) and MPTBh's counterparts.

Experimental Section

Synthesis and Characterization of the Samples. The stability phase domains of phosphate tungsten bronzes $(K_xNa_y)(PO_2)_4(WO_3)_{2m}$ which can be formed within the K−Na−P−W−O system have been established by assuming that the theoretical limit of the K^+ and Na^+ contents is $x + y = 4$ (accounting for X-ray structural data). As a result, the ternary $(PO_2)_4(WO_3)_{2m}$−$Na_4(PO_2)_4(WO_3)_{2m}$−$K_4(PO_2)_4(WO_3)_{2m}$ diagrams have been more investigated particularly for $m = 4$ and $m = 6$. Samples corresponding to various phase compositions were prepared by solid-state reaction from mixtures of $(NH_4)_2HPO_4$, WO_3, W, and alkali metal carbonates following a two-step procedure. First adequate mixtures of $(NH_4)_2HPO_4$, alkali metal carbonates, and WO_3 were heated in a Pt crucible at 600 °C for 24 h to decompose the ammonium phosphate and alkali metal carbonates. Then appropriate amounts of metallic tungsten, used as a reducing agent, were added before the mixtures were fired in sealed silica tubes at 950 °C for 48 h.

The resulting powder samples were characterized by X-ray diffraction analysis using a Philips diffractometer with monochromatized Cu Kα radiation.

Crystal Growth. When necessary, single crystals of the identified phases were grown by chemical vapor transport as described elsewhere.[20] A charge of about 2 g of the powder sample was heated for 2 weeks in a sealed quartz tube (20 cm long and 1.8 cm internal diameter) placed in a two zones furnace 20 cm apart. For the crystal growth experiments, the hot zone was at 1200 °C and the cold zone at 1000 °C. Electron probe microanalysis of the crystals were performed by energy dispersive spectrometry (EDS) using a field emission gun PHILIPS XL30 scanning electron microscope.

Crystal Structure Determination. The quality and the unit cell parameters of the crystals were checked using Weissenberg photographs. X-ray crystal data were collected at 293 K by means of automated ENRAF-NONIUS CAD4 diffractometer with monochromatized Mo Kα radiation.

The background counts were taken at both ends of each $\omega - 2\theta$ scans with ω scan angle = $(1.00 + 0.35 \tan\theta)$. The unit cell was determined from the positions of four alternate settings of 25 reflections with θ between 18° and 25°. Every hour, three intensity control reflections were monitored and used for the slight drift corrections. Intensity data in the range $2.6° \le \theta \le 44.9°$ were corrected for Lorentz and polarization effects and a Gaussian-type correction based on the crystal morphology was applied.

All refinements were performed using the JANA98 program package.[25] Scattering factors for neutral atoms were corrected for anomalous dispersion. All atoms including oxygen were refined with anisotropic displacement parameters.

Electron Transport Measurements. Conventional four-probe dc resistivity measurements were carried out on oriented single crystals. Electrical contacts were made by ultrasonic soldering of indium on the surface of the crystal.

Magnetic susceptibility was measured by means of a SQUID magnetometer using an applied field of 1 T.

Results

Stability Phase Domains. Powder X-ray diffraction data of $(K_xNa_y)(PO_2)_4(WO_3)_{2m}$ samples obtained for $m = 4$ and $m = 6$, and corresponding to different values of both x and y, have been summarized in the ternary diagrams drawn in Figures 1 and 2, respectively. For $m = 4$, only one single-phase domain corresponding to MPTBh's type compounds can be delimited. It shows that this structure is the most stable of the diagram. For $2 < (x + y) \le 4$ the samples are multiphased, involving other members of the series and well-known tungsten bronzes A_xWO_3 (A = Na, K). Furthermore, a small single-phase domain of MPTBp's close to $P_4W_8O_{32}$ could exist but probably with a very small alkali metal solubility ($x + y \le 0.1$).

A similar extended MPTBh's single-phase domain is characterized for $m = 6$ (Figure 2) but with an upper limit of K^+ and Na^+ solubility which can reach $x + y = 3$ higher than that found for $m = 4$ ($x + y = 2$). Moreover

(24) Drouard, S.; Foury, P.; Roussel, P.; Groult, D.; Dumas, J.; Pouget, J. P.; Schlenker, C. *Int. Conf. Synth. Metals −Montpellier-France* **1998**, to be published in *Synthetic Metals*.

(25) Petricek, V.; Dusek, M. *JANA98*; Institute of Physics: Praha; Czech Republic, 1997.

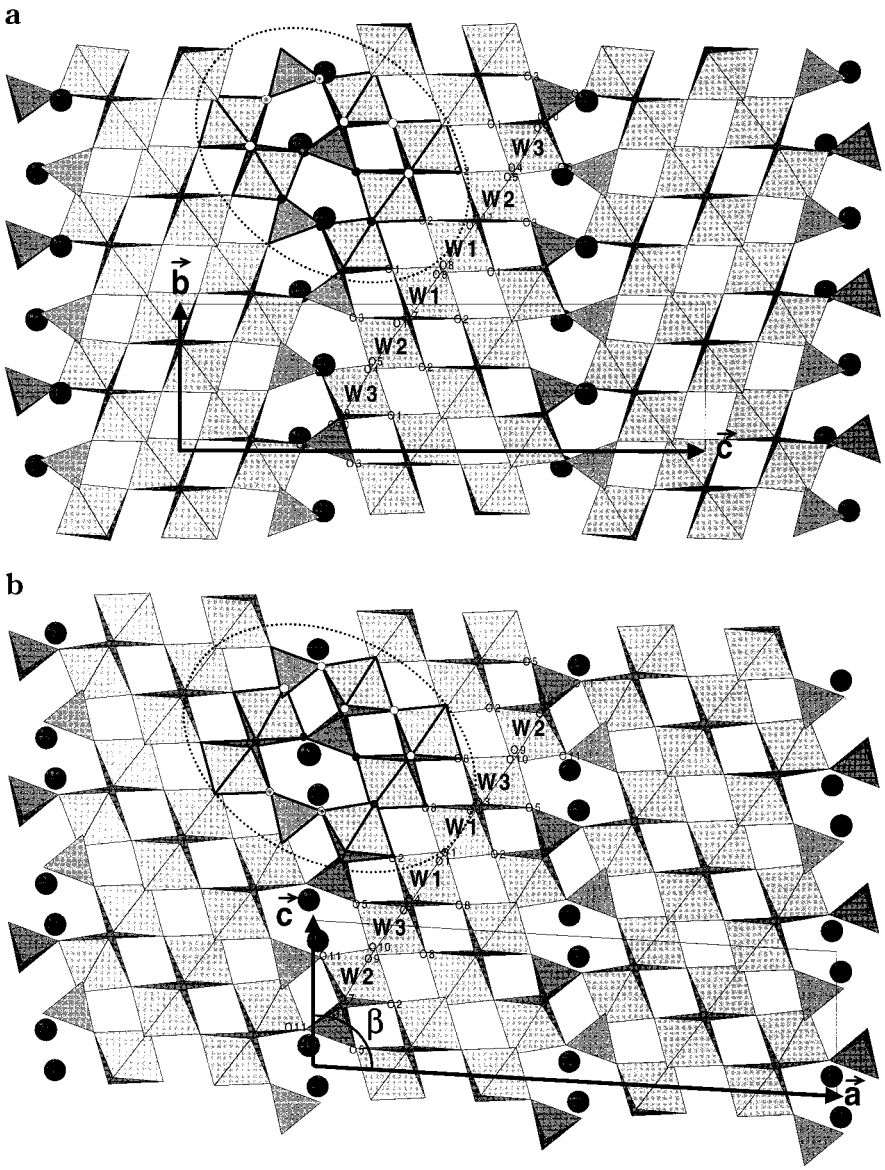

Figure 3. (a) Projection onto (100) of the crystal structure of $Na_{0.96}P_4W_{12}O_{44}$ and (b) onto (010) of the crystal structure of $Na_{1.7}P_4W_{12}O_{44}$. Polyhedra drawn in thick line delimit the extension of O_{18} cages (dotted curves).

the $P_4W_{12}O_{44}$ MPTBp lattice differs from that of $P_4W_8O_{32}$ by its capability to accept a significant amount of Na^+ cations ($0 \leq y \leq 1$) despite similar host Na sites. As a result, a small single-phase domain of $(K_xNa_y)P_4W_{12}O_{44}$ MPTBp's has been delimited for the first time with alkali metal compositions involving Na^+ concentrations higher than K^+ concentrations.

On the other hand, for K^+ concentrations higher than 0.75 ($0.75 \leq x \leq 1.2$), DPTBh $K_xP_4W_{12}O_{44}$-type compounds have been isolated while they are not observed for $m = 4$. Note that insertion of Na^+ in hexagonal tunnels of the diphosphate tungsten bronze structure remains limited to very small concentrations, i.e. less than 10%.

Crystal Structure of the New MPTBp's $Na_{0.96}P_4W_{12}O_{44}$. A crystal with the dimensions 0.26 × 0.19 × 0.06 mm^3 has been selected for data collection at 293 K. Unit cell and X-ray determination parameters are given in Table 1. Similar to $P_4W_{12}O_{44}$,[19] the structure has been refined in orthorhombic symmetry and space group $P2_12_12_1$. A projection of the structure on to (100) has been drawn in Figure 3.

Least-squares refinements based on 2924 observed reflections with $I \geq 3\sigma(I)$ converged to $R = 2.89\%$ (w$R = 4.14\%$) and a goodness of fit = 1.56. The occupancy rate of the Na site is 24(2)%, leading to a content $y = 0.96(8)$ in good agreement with EDS analysis ($y = 0.93$-(4)). Final atomic coordinates and atomic displacements parameters are listed in Tables 2 and 3. Selected interatomic bond distances are given in Table 4.

To make clear the comparison between the structures of $Na_{0.96}P_4W_{12}O_{44}$ (this work) and that of $Na_{1.7}P_4W_{12}O_{44}$ which belongs to the MPTBh's family,[16] the structure of $Na_{1.7}P_4W_{12}O_{44}$ has been sketched in Figure 3b at a same scale as $Na_{0.96}P_4W_{12}O_{44}$.

Resistivity and Magnetic Susceptibility Measurements. Single crystals with sizes as large as 15 × 3 × 0.5 mm^3 have been grown. They have been used for electrical resistance and magnetic susceptibility measurements. The current was always parallel to the *a*,*b* plane.

The temperature dependence of the normalized electrical resistance measured for both MPTBp's and MPTBh's $(K_xNa_y)P_4W_{12}O_{44}$ crystals is shown in Figures 4 and

Table 2. Final Coordinates and Equivalent Isotropic Thermal Parameters[a]

atom	*x*	*y*	*z*	B_{eq} (Å^2)
W1	0.246 50(10)	0.583 93(5)	−0.030 19(1)	0.426(4)
W2	0.257 90(10)	0.761 20(4)	−0.404 02(1)	0.388(4)
W3	0.246 80(10)	0.922 20(4)	−0.158 53(1)	0.361(4)
P	0.262 2(6)	0.115 2(3)	−0.295 60(8)	0.34(3)
O1	0.752(2)	0.257 0(10)	−0.402 2(3)	0.9(1)
O2	0.745(2)	0.085 0(10)	−0.034 7(3)	0.72(9)
O3	0.743(3)	0.423 0(10)	−0.167 0(3)	1.2(1)
O4	0.519 0(10)	0.072 0(10)	−0.138 5(4)	0.7(1)
O5	0.022(2)	0.104 0(10)	−0.130 8(4)	0.6(1)
O6	0.245(3)	0.055 0(10)	−0.233 8(3)	1.1(1)
O7	−0.033(2)	0.431(2)	−0.062 0(4)	0.9(1)
O8	−0.023 0(10)	0.270 0(10)	−0.503 4(4)	0.6(1)
O9	0.041(2)	0.258(2)	−0.309 6(4)	1.1(2)
O10	0.518(2)	0.221(2)	−0.302 1(5)	1.1(2)
O11	0.468(2)	0.406(2)	−0.070 3(3)	0.8(1)
*Na	0.773(4)	0.098(3)	0.773 0(10)	1.3(4)

[a] Starred atom site has a S.O.F. = 0.24(2)

5, respectively. The compositions of the crystals which have been determined by EDS analysis are given in the figures.

For $Na_yP_4W_{12}O_{44}$ MPTBp's (Figure 4), two kinds of electrical resistance behavior can be observed, depending on the Na concentration *y*. For low *y* values ($y \leq 0.1$), the metallic behavior in the normal state is similar to that of the undoped bronze $P_4W_{12}O_{44}$ but becomes different in the low-temperature range. Indeed, while two resistivity anomalies at 120 and 60 K can be noted for $P_4W_{12}O_{44}$, only one anomaly remains at 60 K for $Na_{0.1}P_4W_{12}O_{44}$.[26] For higher *y* values, i.e., $Na_{0.84}P_4W_{12}O_{44}$, the resistivity anomalies have disappeared. (Note that the value $x = 0.1$ of Na concentration corresponds to the upper value which has been estimated from EDS data of three zones of the crystal. It remains at the limit of detection of the method.)

In the case of MPTBh's $K_xP_4W_{12}O_{44}$ and $(K_xNa_y)P_4W_{12}O_{44}$ single crystals (Figure 5), a similar metal behavior is observed down to 4.2 K. However for some crystals corresponding to $x \approx 2$, a change of the slope of the *R* vs *T* curve can be noted below ~140 K. This change appears to be associated with strong positive magnetoresistance effects ($\Delta R/R_0 = 350\%$ at 4.2 K).

As shown in Figure 2, $K_xP_4W_{12}O_{44}$ can also be isolated as DPTBh's for $0.75 \leq x \leq 1.2$. Previous resistivity measurements carried out on a $KP_4W_{12}O_{44}$ crystal[27] attest to the 2D metal behavior. As an example, the *R* vs *T* curve of a crystal having the same composition ($x = 1$) is compared to that of MPTBh's in Figure 5.

Figure 6 shows the temperature dependence of the magnetic susceptibility of $K_{1.82}P_4W_8O_{32}$ and $(K_{0.72}Na_{0.75})P_4W_8O_{32}$ MPTBh's single crystals with the applied magnetic field parallel with the *b* axis. The large drop in the susceptibility at ~150 K observed for the former is consistent with the resistivity data previously reported[23] and assigned to CDW-type transitions. For comparison with the $m = 6$ members of MPTBp, MPTBh and DPTBh's series, typical resistivity curves of $(K_xNa_y)P_4W_8O_{32}$ ($m = 4$) MPTBh's single crystals are shown in Figure 7. Note that for $(K_{1.07},Na_{0.1})P_4W_8O_{32}$ the critical temperature can reach 195 K.

Discussion

Stability phase domains of $(K_xNa_y)(PO_2)_4(WO_3)_{2m}$ phosphate tungsten bronzes have been characterized for $m = 4$ and $m = 6$.

The appearance of a significant MPTBp's single phase domain for $m = 6$, while it does not exist for $m = 4$ is not well understood at present since the alkali metal host sites are similar for both $P_4W_8O_{32}$ and $P_4W_{12}O_{44}$ compounds. A steric effect should be first assumed, due to the difference in size of K^+ and Na^+ cations and the thickness of octahedral WO_3-type slabs. However, as discussed below, it should be pointed out that the pentagonal O_{18} cages which characterize MPTBp's have a volume similar to that of the hexagonal O_{18} cages of MPTBh's which can accommodate equally Na^+ and K^+ ions, whatever the value of *m* may be. On the other hand, such a steric effect can be considered to explain, for K^+, the appearance of DPTBh-type phases because of the large size of hexagonal tunnels which have been demonstrated to accept cations such as K^+, Rb^+, Tl^+, and Ba^{2+}.[12,13]

Comparison between the structures of doped $Na_{0.96}P_4W_{12}O_{44}$ and undoped $P_4W_{12}O_{44}$−MPTBp's shows that both compounds exhibit a similar atomic framework. Only a slight increase of the unit cell parameters can be noted for $Na_{0.96}P_4W_{12}O_{44}$ in agreement with a weak displacement of some diffraction lines on powder XRD patterns. The unit cell volume is thus increased by less than 1% with respect to $P_4W_{12}O_{44}$. This leads to oxygen surroundings of W and P atoms which remain the same in both structures in the limits of three esd's of the W−O and P−O bond distances (Table 4).

The oxygen neighborhood of Na^+ cations in the present MPTBp $Na_{0.96}P_4W_{12}O_{44}$ is compared to that found in the MPTBh $Na_{1.7}P_4W_{12}O_{44}$ in Figure 8. In both types of monophosphates, Na atoms are depicted as being located in O_{18} cages delimited by eight WO_6 octahedra and four PO_4 tetrahedra and having the same size. These cages differ from one another by the shape of the windows by which they communicate (Figure 3). In MPTBp's, each O_{18} cage is related to four equivalent ones by means of pentagonal windows, whereas for MPTBh's each O_{18} cage is related to the next one by means of hexagonal windows. As can be seen in parts a and b of Figure 8, the right parts of both cages are similar contrary to the left parts which can be superimposed only after a binary rotation about a horizontal 2-fold axis. This similarity of the O_{18} cages in MPTBp's and MPTBh's structures suggests that the Na^+ inserted cations should take an identical position with the same oxygen environment. Surprisingly this is not the case. Although the host site is roughly located in the same left part of the cages with eight nearest oxygen atoms, the dispersion of the Na−O bond distances is very different. In MPTBp, the Na atom is 1.50(3) Å off-centered from the gravity center of the cage and has a regular oxygen environment with seven short Na−O bond distances ranging from 2.37(3) Å to 2.64(2) Å and one long Na−O bond distance at 2.82(3) Å. In MPTBh, the Na atom is located at 1.11(5) Å from the gravity center of the O_{18} cage with four short Na−O bond

(26) Roussel, P.; Drouard, S.; Groult, D.; Labbé, Ph.; Dumas, J.; Schlenker, C. *J. Mater. Chem.* **1999**, in press.

(27) Wang, E.; Greenblatt, M.; Rachidi, I. E.; Canadell, E.; Whangbo, M. H. *J. Solid State Chem.* **1989**, *80*, 266.

Table 3. Anisotropic Displacement Parameters[a]

atom	U^{11}	U^{22}	U^{33}	U^{23}	U^{13}	U^{12}
W1	0.0049(1)	0.0054(1)	0.0058(1)	−0.0001(1)	−0.0001(2)	0.0003(2)
W2	0.0041(1)	0.0047(1)	0.0059(1)	0.0000(1)	0.0001(2)	−0.0002(2)
W3	0.0041(1)	0.0046(1)	0.0050(1)	0.0001(1)	0.0000(1)	0.0001(2)
P	0.0042(7)	0.0044(6)	0.0041(5)	0.0015(5)	−0.0003(9)	0.0010(10)
O1	0.014(2)	0.012(2)	0.008(2)	−0.007(2)	0.003(4)	0.003(5)
O2	0.009(2)	0.010(2)	0.008(2)	0.003(2)	0.001(4)	−0.006(4)
O3	0.020(3)	0.010(2)	0.014(2)	0.006(2)	−0.006(4)	0.006(5)
O4	0.005(2)	0.007(3)	0.013(3)	−0.003(3)	−0.002(2)	−0.003(2)
O5	0.008(2)	0.008(3)	0.009(3)	−0.005(2)	0.002(2)	−0.002(3)
O6	0.022(3)	0.014(3)	0.005(2)	0.001(2)	−0.003(4)	−0.011(5)
O7	0.005(2)	0.018(4)	0.010(3)	0.000(3)	0.000(2)	−0.007(3)
O8	0.006(2)	0.006(3)	0.012(3)	0.004(3)	0.001(2)	0.000(3)
O9	0.011(3)	0.014(4)	0.015(3)	0.005(3)	−0.002(3)	0.004(3)
O10	0.008(3)	0.014(4)	0.021(4)	0.008(3)	0.002(3)	−0.003(3)
O11	0.006(2)	0.020(4)	0.006(2)	−0.001(3)	−0.003(2)	0.007(3)
Na	0.004(8)	0.015(8)	0.030(10)	−0.005(8)	−0.007(8)	0.000(8)

[a] The temperature factor has the form of e^{-T} where $T = 2\pi^2\sum_{i,j} h_i h_j U^{ij} a_i^* a_j^*$. a_i^* are reciprocal axial lengths and h_i are the reflection indices.

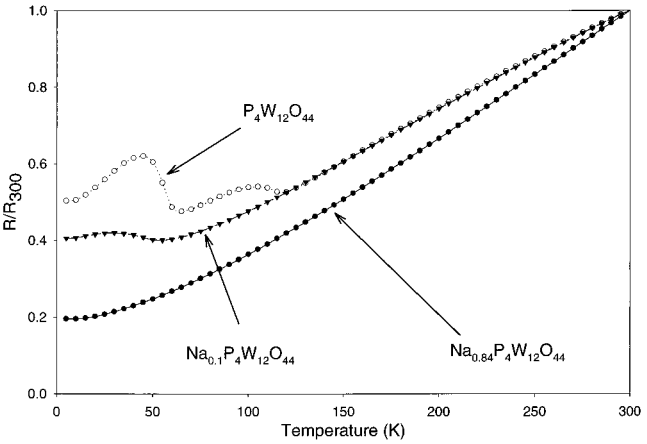

Figure 4. Temperature dependence of the normalized resistance of MPTBp's $P_4W_{12}O_{44}$, $Na_{0.1}P_4W_{12}O_{44}$, and $Na_{0.84}P_4W_{12}O_{44}$ single crystals.

Table 4. Selected Interatomic Distances (Å)

W1−O1	1.962(7)	P−O3	1.543(7)
W1−O2	1.894(7)	P−O6	1.516(7)
W1−O7	1.94(1)	P−O9	1.54(1)
W1−O8	1.865(6)	P−O10	1.53(1)
W1−O8	1.880(7)	Na−O3	2.57(2)
W1−O11	1.91(1)	Na−O4	2.49(2)
W2−O2	1.855(7)	Na−O5	2.63(3)
W2−O3	1.988(7)	Na−O6	2.82(3)
W2−O4	1.990(7)	Na−O6	2.53(3)
W2−O5	1.989(9)	Na−O9	2.64(2)
W2−O7	1.82(1)	Na−O9	2.59(2)
W2−O11	1.84(1)	Na−O10	2.37(3)
W3−O1	1.801(7)		
W3−O4	1.812(6)		
W3−O5	1.812(9)		
W3−O6	1.982(7)		
W3−O9	2.02(1)		
W3−O10	2.04(1)		

distances between 2.45(4) Å and 2.64(5) Å and four longer ones between 2.85(3) Å and 3.02(3) Å.

Because of the separation of the conducting WO_3-type layers by insulating phosphate slices and of the preferential delocalization of conduction electrons on chains of WO_6 octahedra, low dimensional metallic properties are observed for both DPTB's and MPTB's in the normal state. A factor of roughly 3 is found for the anisotropy of room-temperature resistivity between the in-plane and perpendicular directions of the crystals. Magnetic susceptibility measurements are consistent with the resistivity data, showing a temperature independent Pauli paramagnetic behavior (Figure 6).

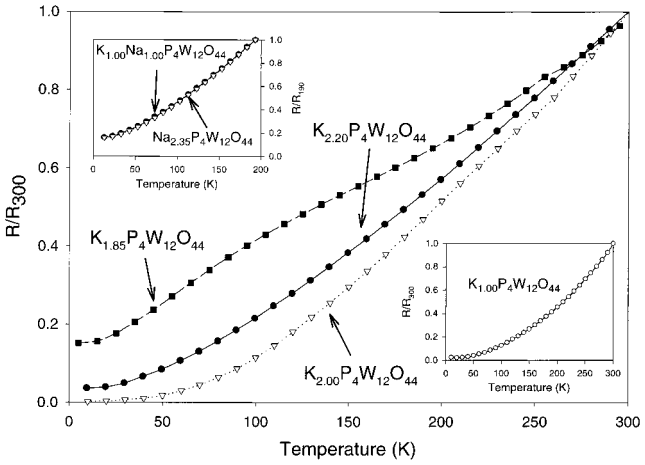

Figure 5. Temperature dependence of the normalized resistance of MPTBh's $K_xP_4W_{12}O_{44}$ single crystals. In the inserts are represented the R vs T curves for MPTBh's $Na_{2.35}P_4W_{12}O_{44}$ and $(K_{1.00}Na_{1.00})P_4W_{12}O_{44}$ (upper left) and for DPTBh's $K_{1.00}$-$P_4W_{12}O_{44}$ (lower right)

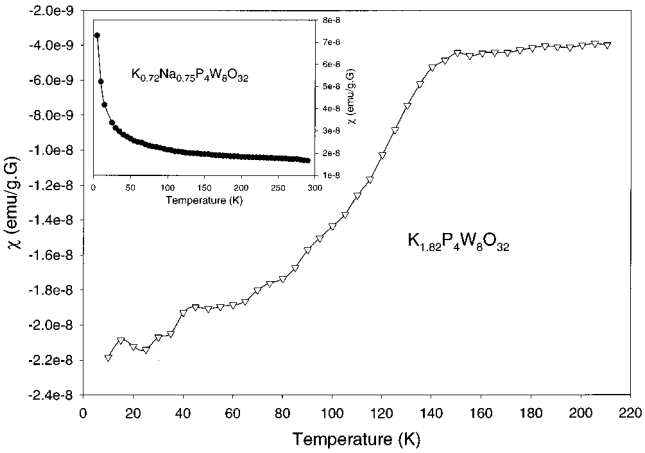

Figure 6. Temperature dependence of the magnetic susceptibility of single crystals $K_{1.82}P_4W_8O_{32}$ and $K_{0.72}Na_{0.75}P_4W_8O_{32}$.

At low temperature, a large drop in the susceptibility is observed for $K_xP_4W_8O_{32}$ MPTBh's which could be due to a decrease of charge carrier density and a partial destruction of FS possibly related to a CDW gap opening as described for undoped MPTBp's $(PO_2)_4(WO_3)_{2m}$.[3] On

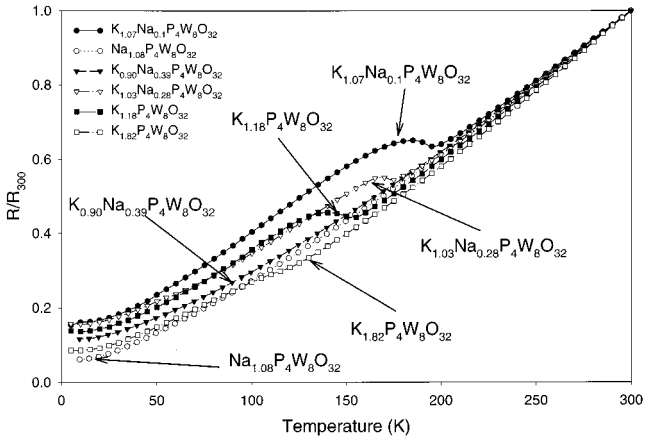

Figure 7. Temperature dependence of the normalized resistance of MPTBh's $(K_xNa_y)P_4W_8O_{32}$ single crystals.

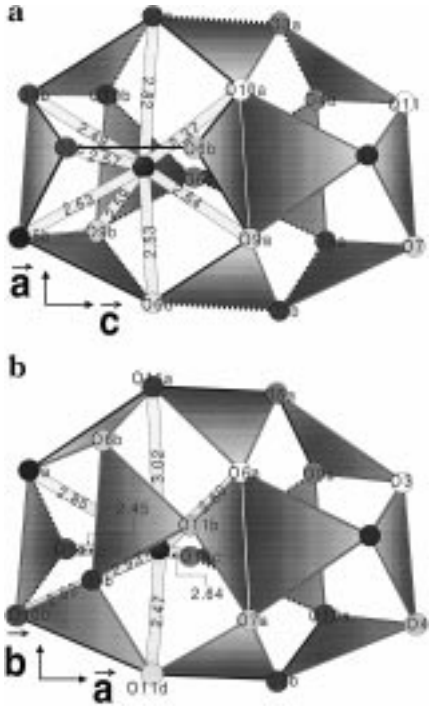

Figure 8. Location of the Na^+ cation inside a O_{18} cage: (a) in the MPTBp $Na_{0.96}P_4W_{12}O_{44}$ (this work) and (b) in the MPTBh $Na_{1.7}P_4W_{12}O_{44}$ (ref 16). Observe that the left parts of the cages can be superimposed after a binary rotation about an horizontal 2-fold axis.

the basis of the resistivity data obtained for $K_xP_4W_8O_{32}$[24] it seems that a minimum of 0.60 electron per W atom is needed for the appearance of a visible metal-to-metal transition. Upon varying the potassium content, x, between 0.8 and 2.0, the critical temperature of this transition reaches a maximum value $T_c \approx 170$ K for $x \approx 4/3$. According to band structure calculations carried out for $K_{0.8}P_4W_8O_{32}$,[7] this value $x \approx 1.33$ which corresponds to 0.66 electron per W atom would result in a maximum of the density of state at the Fermi level, possibly related to two-half filled and one empty conduction bands.

The absence of similar resistivity anomalies for $K_xP_4W_{12}O_{44}$ MPTBh's might be due to several reasons involving *(i)* the quality of the samples through the existence of structural defects and/or impurities, *(ii)* the potassium ordering in the O_{18} cages, *(iii)* the electron band filling and/or the topology of the Fermi surface.

According to previous HREM observations,[28] it indeed appears rather difficult to find a perfectly regular crystal, especially when m increases, although the ED patterns look perfect. WO_3-type slabs with a thickness different from that of the expected matrix are frequently observed, so involving more or less extended intergrowth defects. Moreover, stopping and shifting of phosphate rows due to the replacement of PO_4 tetrahedra by WO_6 octahedra can lead to numerous isolated defects.

Potassium occupation variations of O_{18} cages characterized by the appearance of extra spots on ED patterns and contrast variations of the tunnel rows on HREM images can also play a major role as more recently shown from X-ray diffuse scattering experiments performed on $K_xP_4W_8O_{32}$ crystals with $x \approx 2$.[24]

Besides such induced order−disorder phenomena, K^+ cations change the number of conduction electrons ($n = 2 + x/2$) per unit cell, i.e., the electron band filling. Therefore a change of FS topologies and nesting properties can be assumed as demonstrated from band structure calculations.

For the Na-based MPTBh's counterparts no anomalies in resistivity (this work), thermopower and Hall constant measurements[29] have been clearly detected. However, it should be noted here that weak and broad metal-to-metal transitions observable at ∼90 and ∼140 K on resistivity curves have been reported by Wang et al.[30] for $Na_{1.6}P_4W_8O_{32}$ and $Na_2P_4W_{12}O_{44}$ crystals oriented along the predominant direction of conductivity (b axis). The differences in electrical behavior between Na-based MPTBh and K-based analogues could be due to the difference in crystal symmetry and then in FS topology. Indeed the structures of $Na_{1.5}P_4W_8O_{32}$ and $Na_{1.7}P_4W_{12}O_{44}$ have been shown to differ from that of $K_{0.84}P_4W_8O_{32}$ and $K_{2.00}P_4W_{12}O_{44}$ by a tilting of about 8° of the WO_6 octahedra so that two adjacent WO_3-type slabs are no longer equivalent from a translation. This implies a doubling of the c parameter and a lowering of crystal symmetry.

In contrast, for the new MPTBp's phase $Na_yP_4W_{12}O_{44}$ which has been isolated for $0 \leq y \leq 1$, the structure remains close to that of the undoped compound $P_4W_{12}O_{44}$ with no change of crystal symmetry. As a consequence, the fact that the CDW transitions at $T_{c1} = 120$ K and $T_{c2} = 60$ K (Figure 4) disappear one after the other as the doping rate y increases might be explained on the basis of Na^+-induced random potentials which are known to hinder and/or prevent CDW formation.

Conclusion

The aim of the present work was to clearly define the stability phase domains of phosphate tungsten bronzes $(K_xNa_y)(PO_2)_4(WO_3)_{2m}$ belonging to the DPTBh, MPTBh, and MPTBp's series which can be formed within the K−Na−P−W−O system.

The two values $m = 4$ and $m = 6$ of the thickness parameter m have been specially investigated. The nature of the phases which can be obtained has been

(28) Domengès, B.; Hervieu, M.; Raveau, B.; O'Keeffe, M. *J. Solid State Chem.* **1988**, *72*, 155.
(29) Drouard, S.; Schlenker, C. Private communication.
(30) Wang E.; Greenblatt M.; Rachidi, I. E.; Canadell, E.; Whangbo, M. H. *J. Solid State Chem.* **1989**, *81*, 173.
(31) Becker, P. J.; Coppens, P. *Acta Crystallogr.* **1974**, *A30*, 148.

reported on ternary diagrams as a function of the concentrations of Na^+ and K^+ cations in the starting materials.

For $m = 4$, the stability phase domain of the MPTBh family is the most important which implies that the structure first described for $K_{0.84}P_4W_8O_{32}$[15] and $Na_{1.5}P_4W_8O_{32}$[16] is the most stable of the diagram. It corresponds for $K_xP_4W_8O_{32}$ to a doping rate ranging from 0.75 to 2.0 which does not significantly change for mixed $(K_x,Na_y)P_4W_8O_{32}$ samples. On the other hand, the relative concentrations of K^+ and Na^+ cations in the crystals seem to play a crucial role for the appearance of CDW-type instabilities which can indeed be detected for $x \geq 2.5y$.

For $m = 6$, the results show that the MPTBh structure also exhibits the most extended stability phase domain with a composition range corresponding to $1.3 \leq x \leq 2.8$ for K-based compounds and $1.2 \leq y \leq 3.0$ for Na-based compounds. In the past, only one composition, $Na_{1.7}P_4W_{12}O_{44}$, has been described from structural investigations.[16] More recently the structure of $K_2P_4W_{12}O_{44}$ has been solved from X-ray diffraction data.[26]

Compared to $m = 4$, the ternary diagram drawn for $m = 6$ gives evidence of two additional stability phase domains. They correspond to compositions which involve K^+ concentrations higher than Na^+ for the former and Na^+ concentrations higher than K^+ for the latter and to structures which are related to those of the DPTBh and MPTBp series, respectively.

$Na_yP_4W_{12}O_{44}$ samples belonging to the MPTBp family with $0 < y \leq 1$ have thus been synthesized for the first time. The structure of $Na_{0.96}P_4W_{12}O_{44}$ has been solved and compared to that of the MPTBh counterpart $Na_{1.7}P_4W_{12}O_{44}$. A preliminary study of the electron transport properties suggests that the 120 K transition seen in $P_4W_{12}O_{44}$ is gone as $y = 0.1$ while the 120 and 60 K transitions are destroyed as $y \approx 1$. Further physical measurements on crystals corresponding to different values of y is necessary in order to obtain a clearer understanding of electronic instabilities in doped monophosphate tungsten bronzes including both MPTBp and MPTBh.

Supporting Information Available: Details of structure determination (in CIF format) and structure factor tables for $Na_{0.96}P_4W_{12}O_{44}$. This material is available free of charge via the Internet at http://pubs.acs.org.

CM9807790